

## GRACE-derived land-hydrological mass changes and their impact on relative sea-level variations



Oliver Baur, Michael Kuhn and Will E. Featherstone

### Abstract

The GRACE (Gravity Recovery And Climate Experiment) mission allows inference of mass variations on, above and beneath the Earth's surface from gravitational signatures in space. We present a robust and straightforward procedure to derive mass changes from time-variable gravity field estimates. We outline our solution to the leakage problem and shed light on linear versus accelerated secular-change modeling. Based on a six-year gravity field time-series from March 2003 to February 2009, we provide detailed analysis of two selected areas, Greenland and the Orinoco Basin. As a result, annual Greenland mass loss accelerated by  $+21.3 \pm 3 \text{ Gt/yr}^2$  during the six-year period. Furthermore, we show the impact of recent ice melting on global relative sea level. In terms of uniform change, the contributions of Greenland and Antarctica are  $+0.56 \pm 0.01 \text{ mm/yr}$  and  $+0.50 \pm 0.07 \text{ mm/yr}$ , respectively. However, we prove that simplistic uniform modeling of sea-level variations is insufficient as it disregards the gravitational feedback effect caused by mass redistribution.

**Keywords:** Satellite gravimetry, mass balance, trend estimation, sea-level change

### Kurzfassung

Mit dem Start der Satellitenmission GRACE (Gravity Recovery And Climate Experiment) wurde es erstmals möglich, großräumige Massenvariationen im System Erde aus Änderungen in der Erdanziehungskraft zu bestimmen. Im Rahmen der Klimawandeldebatte nimmt dabei der anhaltende Eismassenverlust in den polaren Gebieten der Erde eine besonders bedeutende Stellung ein. Dieser Beitrag präsentiert eine robuste und geradlinige Vorgehensweise zur Bestimmung von Massenänderungen aus zeitvariablen Schwerefeldern. In diesem Zusammenhang spielt der Umgang mit Kriecheffekten (leakage) eine maßgebliche Rolle. Darüber hinaus widmen wir uns der Frage, auf welche Art und Weise der säkulare Trend in den Zeitreihen modelliert werden sollte. Unsere Analyse einer Serie monatlicher Schwerefelder über den Zeitraum März 2003 bis Februar 2009 zeigt, dass sich der jährliche Eismassenschwund über Grönland mit einer Rate von  $+21.3 \pm 3 \text{ Gt/yr}^2$  beschleunigt hat. Das Resultat zunehmender Eisschmelze erweist sich als signifikant im Rahmen der durchgeführten statistischen Tests. Der Zufluss von Schmelzwasser in die Ozeane bedingt naturgemäß einen Anstieg des Meeresspiegels. Ausgedrückt in räumlich gleichförmiger Ausprägung liefern Grönland und die Antarktis mit  $+0.56 \pm 0.01 \text{ mm/yr}$  beziehungsweise  $+0.50 \pm 0.07 \text{ mm/yr}$  derzeit den primären Beitrag. Die Annahme einer auf die Ozeane aufgetragenen konstanten Schicht ist indessen ungenügend. Aufgrund der globalen Massen-Neuverteilung resultiert eine regional sehr unterschiedlich ausgeprägte Variation des relativen Meeresspiegels. Aus diesem Grund müssen sowohl der gravitative Rückkopplungseffekt als auch der Auflasteffekt berücksichtigt werden.

**Schlüsselwörter:** Satellitengravimetrie, Massenbilanz, Trendschätzung, Meeresspiegel

### 1. Introduction

In the context of climate change, the Gravity Recovery And Climate Experiment (GRACE) provides valuable information on mass transport in the system Earth [1]. Range-rate measurements collected by the twin-satellite mission are particularly sensitive to mass variations over large-scale regions. The spacecraft are some nine years in operational mode now. Nevertheless, climate-change forecasts remain a matter of contention. Considering decadal and longer-term variations, the GRACE lifetime is too short to derive statistically meaningful predictions from the data.

GRACE gravity field time-series have often been exploited to determine linear ablation rates in glaciated areas such as Greenland [2], Alaska [3], Antarctica [4] and Patagonia [5]. Hydrological studies typically target seasonal mass-variation characteristics of river basins and water catchments [1,6]. In the recent past, two issues gained increasing interest. Firstly, the more detailed spatial resolution of mass change patterns; [7,8], for instance, subdivided the Greenland area in catchments to improve spatial variability. In [9], point-mass modeling is used to recover the deglaciation geometry. Secondly, it has been shown that linear mass-change trends may in-

adequately represent the temporal progress of secular variations. [10] found that Greenland ice-mass loss accelerated by about 250% between April 2002 to April 2004 and May 2004 to April 2006. This result was supported by [11], analyzing a seven-year period and applying various metric criteria. [12] suggest that over the last 18 years, deglaciation over Greenland and Antarctica accelerated by  $+21.9 \pm 1 \text{ Gt/yr}^2$  and  $+14.5 \pm 2 \text{ Gt/yr}^2$ , respectively.

The motivation of this contribution is twofold. On the one hand, we present a procedure to derive mass-change rates from GRACE gravity field time-series. We (i) shed light on the leakage problem inherent to GRACE analysis, (ii) briefly address glacial isostatic adjustment (GIA) corrections, and (iii) discuss the modeling of secular trends. On the other hand, we translate land-hydrological mass changes to equivalent (relative) sea-level variations. In this framework, we exclusively modeled non-steric changes as GRACE is only sensitive to sea-level variations related to gravitational signatures. [The steric component, mainly driven by thermal expansion, is typically obtained from a combination with satellite altimetry and in-situ observation systems such as Argo. For detailed information, we refer the reader to [13] and the references therein]. Opposed to the simplified assumption of uniform change geometries, regional patterns strongly contradict the constant-layer approximation; we adopted the theory in [14] to take both the gravitational and elastic feedback effects into account.

## 2. GRACE-derived mass changes

Section 2.1 introduces the data used for this study. The methods section 2.2 outlines our algorithms to compute mass-change rates from GRACE gravity fields; we refer the reader to [11] and [15] for a detailed description of the techniques. Finally, exemplary for any region of interest, Sect. 2.3 presents results for Greenland and the Orinoco Basin.

### 2.1 Data

GRACE gravity field time-series are provided by several data processing centers. For our experiments, we used the well-established release RL04 estimates from the Center for Space Research (CSR) at the University of Texas at Austin. Each "monthly" solution consists of a set of fully normalized spherical harmonic coefficients (SHC) complete up to degree ( $l$ ) and order ( $m$ ) 60. The time period for this study covers March 2003 to February 2009, hence six integer years. Satel-

lite gravimetry is insensitive to displacements of the Earth's centre of mass; for this reason, the monthly solutions do not contain degree-1 coefficients. The neglect of secular geocenter motions, such as caused by GIA [16], might introduce a bias to mass-change estimates. As reported by [17], geocenter adjustment over the period July 2003 to June 2007 resulted in approximately  $+0.2 \text{ mm/yr}$  uniform sea-level change equivalent. We replaced GRACE  $c_{20}$  coefficients (representing the Earth's flattening) by values based on satellite laser ranging, which have been proven to be more reliable [18].

### 2.2 Methods

Vertically integrated mass variations, as sensed by GRACE, are commonly approximated by surface mass densities [19]. In terms of equivalent water height (EWH), the changes become

$$\begin{aligned} \Delta \text{EHW}(\lambda, \varphi) &= \\ &= \frac{2\pi a \rho_{\text{ave}}}{3\rho_w} \sum_{l=2}^L \frac{2l+1}{1+k_l} W_l \cdot \\ &\quad \cdot \sum_{m=0}^l P_{lm}(\sin \varphi) [\Delta c_{lm}^{\text{fil}} \cos(m\lambda) + \Delta s_{lm}^{\text{fil}} \sin(m\lambda)] \end{aligned} \quad (1)$$

where  $\Delta c_{lm}^{\text{fil}}$  and  $\Delta s_{lm}^{\text{fil}}$  denote residual SHC taken with respect to the (assumed static) six-year means. The superscript fil indicates that we removed systematic errors by spectral-domain filtering as proposed in [20]. The degree-dependent factors  $W_l$  down-weight short-wavelength features, which are prone to GRACE errors. We selected the factors according to isotropic Gaussian smoothing with a radius of 500 km [21].

In Eq. (1),  $\lambda$  and  $\varphi$  represent longitude and latitude, respectively;  $a$  is the major semi-axis of a reference ellipsoid,  $\rho_{\text{ave}}$  the average mass-density of the solid Earth,  $\rho_w$  the mass-density of freshwater,  $L = l_{\text{max}}$  (here  $L = 60$ ) the maximum spherical harmonic degree and  $k_l$  the load Love numbers. The  $P_{lm}(\sin \varphi)$  are the normalized associated Legendre functions of the first kind.

Based on monthly "snapshots" of residual EWH patterns, Fig. 1 shows global trends from March 2003 to February 2009. The signals over Greenland, Alaska and Antarctica can be attributed to cryospheric processes, whereas the signals over the Canadian Shield and Fennoscandia are mainly subject to GIA. Furthermore, Fig. 1 reveals secular (surface- and ground-water) changes in large river catchments such as the Orinoco Basin and the Mississippi Basin. Noteworthy, it is a delicate matter to separate between real mass-change signals and spurious signals triggered by GRACE errors. Geophysical

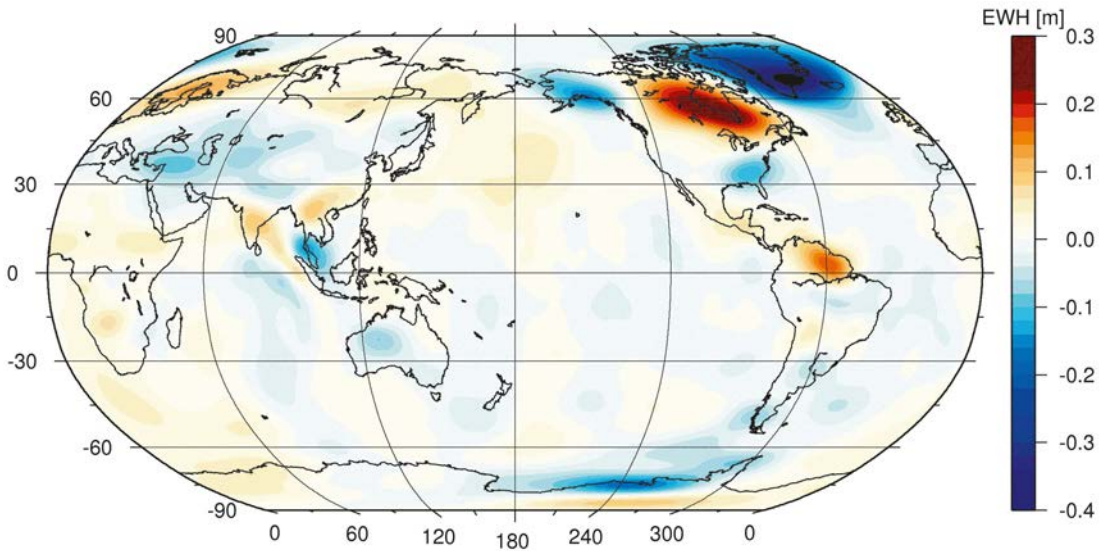


Fig. 1: Secular trends from GRACE gravimetry in terms of EWH. Pattern extracted from the CSR gravity field time-series from March 2003 to February 2009. At each point of a global  $1^\circ \times 1^\circ$  grid a regression line was fit to the time series of residual EWH values, cf. Eq. (1).

interpretation of minor features, hence, has to be done with care.

### 2.2.1 Removing leakage

A major challenge to deriving reliable mass changes from GRACE manifests in the correction for leakage effects. Leakage occurs due to both the restricted spectral resolution ( $L \ll \infty$ ) of gravitational field estimates and spatial averaging in terms of Gaussian smoothing. We demonstrate the situation by means of a simple synthetic example. We assume a disc-shaped mass anomaly of radius  $10^\circ$  located on the Earth's surface (cf. Fig. 2). The disc's gravitational signal is assessed by potential forward modeling (Newton integration). In order to recover the initial mass anomaly from its gravitational attrac-

tion, we truncated the spherical harmonic series at degree and order 60 and applied Gaussian smoothing with a radius of 500 km. Hence, the simulated scenario is consistent with our GRACE analysis.

Only 71% of the initial total mass is located within the disc-shaped area (Fig. 2). From the disc-shaped area point of view, 29% of the signal leaks out. On the other hand, from the perspective of an area outside the disc, signal leaks in. Whereas leakage-out signals have to be restored back into the region of interest, leakage-in signals have to be reduced from it. Although leakage signals strongly attenuate with increasing distance from the source, GRACE mass-change estimates are highly sensitive to these disturbing effects. The signal over Greenland, for instance,

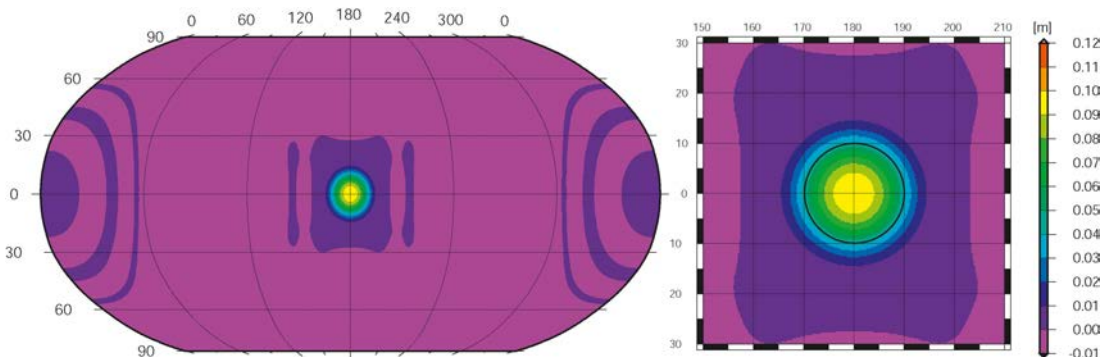


Fig. 2: Signal leakage experiment based on a simulated disc-shaped mass anomaly. The disc with a radius of  $10^\circ$  and 0.1 m EWH value is located on the equator at  $180^\circ$  E. 29% of the gravitational signal leaks out of the initial area.

spreads out over the whole globe. At the same time, signal over the Canadian Shield leaks into the Greenland area (cf. Fig. 1).

We developed and applied a robust four-step procedure to determine mass change from leakage-affected GRACE patterns, cf. [15]. The procedure isolates and quantifies both leakage-out signals and leakage-in signals. The method is a combination of extended spatial filters, followed by “calibration” in terms of comparison with forward gravity field modeling.

### 2.2.2 Glacial isostatic adjustment

GRACE is sensitive to vertically integrated mass variations, hence does not allow for the detection of their vertical (re)distribution. Post glacial rebound signals, in particular, distort conclusions on the magnitudes of contemporary mass transport. GIA modeling is highly subject to assumptions of ice-load history and mantle viscosity. For this reason, independent models differ significantly. As an example, [22] showed that the GIA contribution over Antarctica amounts to  $+100 \pm 67$  Gt/yr. In contrast, [4] quantified the change rate to  $+176 \pm 72$  Gt/yr. Here we used the GIA model according to [23] (Fig. 3), following the recommendation by the GRACE Tellus Team ([grace.jpl.nasa.gov](http://grace.jpl.nasa.gov)).

### 2.2.3 Modeling of secular trends

In order to avoid aliasing effects of strong seasonal signals falsifying our secular-change estimates, we fit basin-averaged residual mass-change time-series with a polynomial and three sinusoids, namely the annual signal, semi-annual signal and a 161-day tidal alias [24]. The model equation is

$$y(t_i) = \sum_{j=0}^n p_j t_i^j + \sum_{k=1}^3 A_k \cos(2\pi f_k t_i) + \sum_{k=1}^3 B_k \sin(2\pi f_k t_i) \quad i = 1, \dots, u. \quad (2)$$

The first term in Eq. (2) represents the secular trend (in terms of polynomial coefficients  $p_j$ ). Here, we investigate linear ( $n=1$ ) versus accelerated ( $n=2$ ) processes.  $y(t_i)$  denote residual mass changes at time  $t_i$ ,  $f_k$  are pre-defined frequencies according to the modeled sinusoids,  $A_k$  and  $B_k$  are the corresponding amplitudes.

We judged appropriate secular-trend modeling on the basis of the statistical significance of the estimated regression parameters. In particular, we balanced the null hypothesis  $H_0: p_j=0$  against the alternative hypothesis  $H_1: p_j \neq 0$ ; results of the Student-test are subject to a 95% confidence interval.

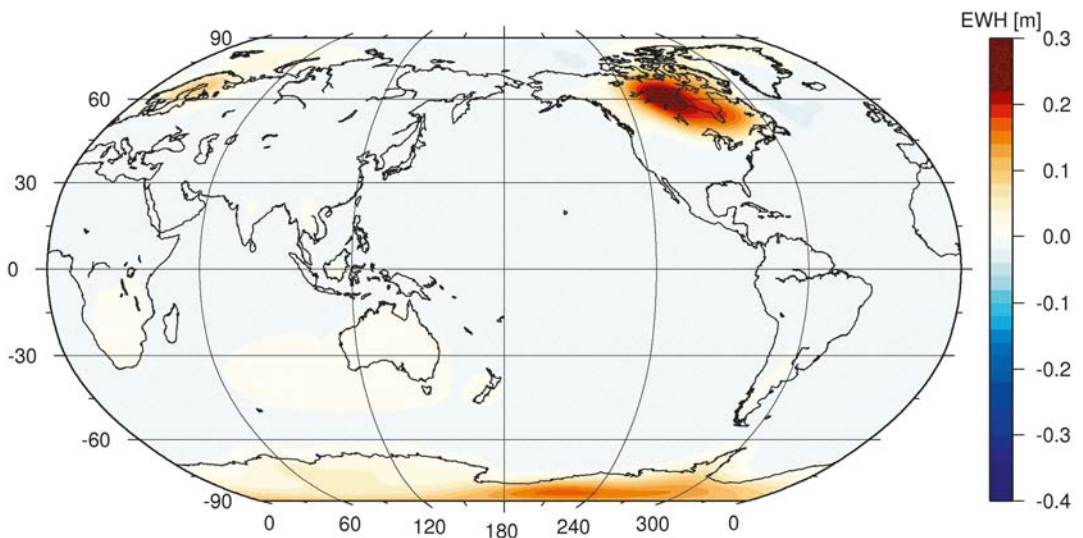
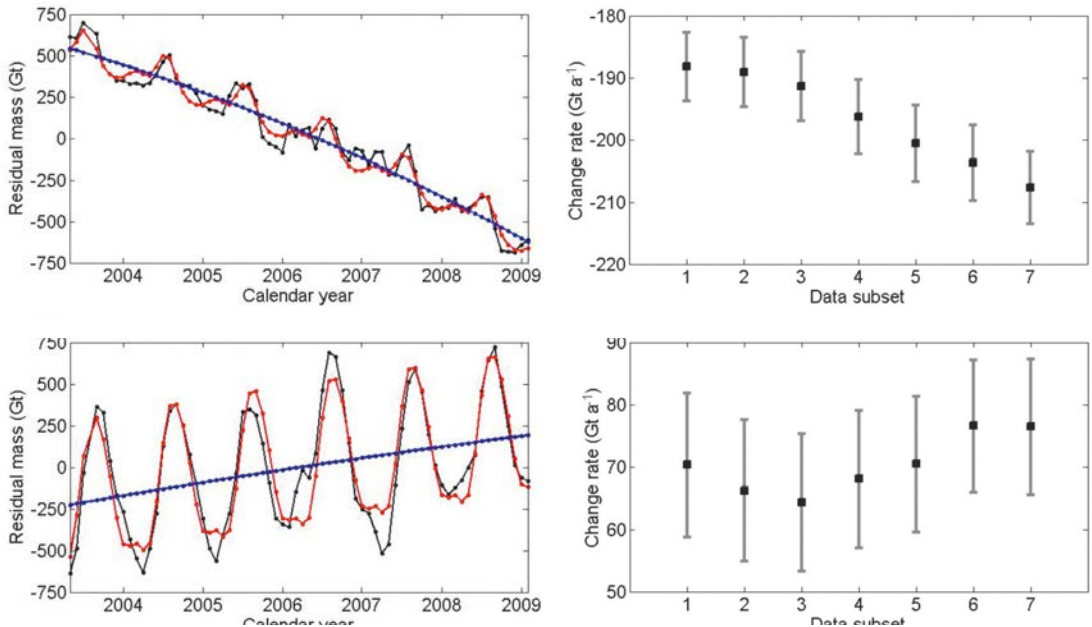


Fig. 3: GIA-induced mass-variation signal in terms of EWH. Pattern extracted from the GIA model in [23] over a six-year period. Within short periods, the GIA signal can be assumed to be linear in time. The same scale as in Fig. 1 applies. A comparison of the patterns reveals that the GRACE signals over the Canadian Shield and Fennoscandia are mainly caused by the rebound effect. Most of the GIA signal over Antarctica is balanced by the deglaciation signal.



**Fig. 4:** Greenland (left panels) and Orinoco Basin (right panels) mass variations from March 2003 to February 2009 (no GIA corrections applied). Top: black lines – monthly residual mass with respect to the temporal mean; red lines – least-squares fit ( $n=2$ ) according to Eq. (2); blue lines – least-squares fit ( $n=2$ ) according to Eq. (2), reduced by seasonal signals. Bottom: linear change rates taken over five-year data subsets. Each subset has an offset of two months to the previous one. Error bars indicate the standard deviation of the estimates.

### 2.3 Results

Fig. 4 (top panels) presents time series of residual mass taken with respect to long-term averages. Whereas Greenland is mainly affected by secular mass loss, in the Orinoco Basin seasonal variations dominate. Most notably, for Greenland we found linear change-rate modeling to be insufficient. Indeed, mass loss increased by  $+21.3 \pm 3 \text{ Gt/yr}^2$ . Greenland, thus, undergoes accelerated ice melting in the six-year time-period considered. Using a second-order polynomial fit, the total loss over the six-year period amounts to  $+1167 \pm 18 \text{ Gt}$ . For the Orinoco Basin, hypothesis testing proved linear regression to be superior to a quadratic fit. Over the period of investigation, the basin gained water at a rate of  $+75 \pm 9 \text{ Gt/yr}$  (i.e., no acceleration).

These findings are supported by the results displayed in the bottom panels in Fig. 4. For Greenland, the slopes of linear regression lines derived over various five-year data subsets increase significantly. Variations of change rates in the Orinoco Basin, on the other hand, are within the error bounds, i.e., not meaningful from a statistical point of view.

### 3. Sea-level change equivalent

Land-hydrological mass variations directly impact global sea-level change (SLC). Eustatic modeling translates mass gain or loss over land area to uniform water changes over the oceans. However, instead of resulting in globally uniform sea-level variations, the (re)distribution of water is spatially variable, which is due to the gravitational and elastic feedback effects caused by the changing surface mass geometries and loads.

Noteworthy, regional patterns subject to specific environmental constraints may significantly deviate from global modeling. For this reason, the conclusions drawn in this section have to be considered in a more general context. In Sect. 3.1, we shed light on the basic methodology of SLC forward modeling, following the theory in [14]. Section 3.2 presents selected results. In particular, we focus on the polar regions of the Earth, which contemporarily show the strongest (GIA-corrected) signals; that is, the secular mass trends as observed by GRACE (cf. Fig. 1) have been corrected by the GIA-signal shown in Fig. 3 so to only represent [assumed] hydrological changes.

### 3.1 Methods

Taking the gravitational and elastic feedback effects into account, the spatial dependency of the new relative sea level  $S(\lambda, \varphi)$  is given by

$$S(\lambda, \varphi) = S_{ii} + [S_{\Delta\Phi}(\lambda, \varphi) - \langle S_{\Delta\Phi}(\lambda, \varphi) \rangle_o] + [U_e(\lambda, \varphi) - \langle U_e(\lambda, \varphi) \rangle_o] \quad (3)$$

where  $S_{ii}$  denotes the global average of all residual water masses. The SLC caused by the gravitational feedback effect of the changing masses is given by  $S_{\Delta\Phi}(\lambda, \varphi) = \Delta\Phi(\lambda, \varphi) / g$ ; therein,  $\Delta\Phi(\lambda, \varphi)$  represents the change in the Earth's gravitational potential (including the elastic feedback) and  $g$  is the gravitational acceleration on the Earth's surface. The vertical surface displacement due to the elastic response is expressed by  $U_e(\lambda, \varphi)$ , i.e., Eq. (3) models sea-level relative to the changing surface of the Earth. The integral-averages  $\langle S_{\Delta\Phi}(\lambda, \varphi) \rangle_o$  and  $\langle U_e(\lambda, \varphi) \rangle_o$  are taken over the global ocean area and have to be subtracted so that the total mass-variation magnitude over the oceans corresponds to the uniform change, i.e.,  $\langle S(\lambda, \varphi) \rangle_o = S_{ii}$ . Equation (3) has to be solved iteratively as both  $\Delta\Phi(\lambda, \varphi)$  and  $U_e(\lambda, \varphi)$  require knowledge of  $S(\lambda, \varphi)$ .

Noteworthy, the new sea-level surface follows that particular equipotential surface in the changed Earth's gravitational field that preserves the eustatic change in a global average sense. Consequently, real sea-level variations are always lower than the eustatic change close to mass-loss areas and higher than the eustatic change further away from them [14,25,26]. Opposite effects hold for mass-accumulation areas.

### 3.2 Results

We applied SLC forward modeling to Greenland and Antarctic mass changes, i.e., to areas with most dominant (GIA-corrected) hydrological signals as detected by GRACE. As such, we shed light on contemporary deglaciation-induced relative sea-level rise. Fig. 5 reveals that relative

sea level does not change in a uniform manner. Most notably, in offshore regions near land ice-mass loss, sea-level fall can be observed. Greenland-induced SLC varies between  $-3$  mm/yr and  $+1$  mm/yr; the average is  $+0.56$  mm/yr. The minimum and maximum values for Antarctica are  $-1.0$  mm/yr and  $+1.0$  mm/yr, respectively; the average amounts to  $+0.50$  mm/yr.

Ice melting in the Arctic mainly causes sea-level rise in the Southern Hemisphere; ice loss over Antarctica dominates sea-level rise in the Northern Hemisphere. As a consequence, the combined pattern is close to the eustatic scenario for vast areas of the world's oceans. However, most regions above 30N and below a 60S are affected less than the eustatic change. The maximum relative sea-level rise is present mostly along a belt covering the tropics and subtropics.

### 4. Conclusions

From our simulation experiments and GRACE results, we claim to have a comprehensive toolkit at hand that allows reliable gravity-related studies on mass transport in the system Earth. Both total mass-change numbers within certain time periods and the temporal progress of these changes are of utmost importance to improve the understanding of present-day phenomena. In this context, we confirm accelerated Greenland ice loss as reported in [12]. Although the numbers are astonishingly close to each other ( $+21.9 \pm 1$  Gt/yr<sup>2</sup> versus  $+21.3 \pm 3$  Gt/yr<sup>2</sup>), the rates refer to different periods, so should not be compared directly.

The error bounds we provide are derived from residuals between the recovered mass-variation time series and the least-squares fit to this series; they do not account for the uncertainties of SHC, and hence GRACE errors. A more rigorous approach would include spectral-to-spatial domain error propagation. In this framework, SHC (co)variance scaling would need to be investigated in order to account for realistic noise levels. Although

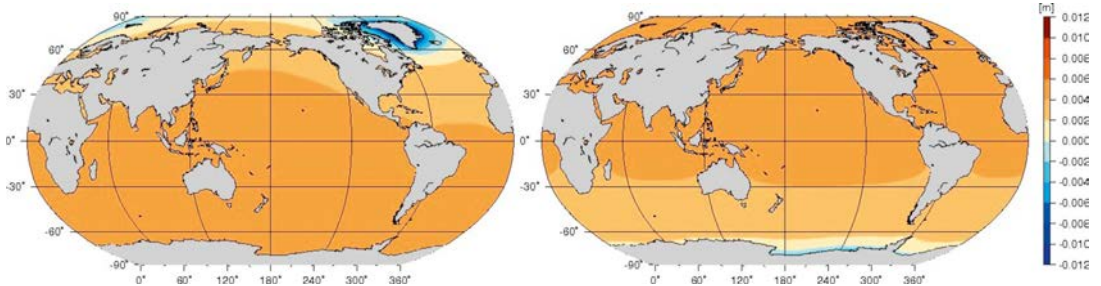


Fig. 5: Global SLC from Greenland (left panel) and Antarctica (right panel) mass-change geometries; GIA corrections applied. Patterns hold for a seven-year period, taking gravitational and elastic feedback effects into account.

we are aware of the fact that our error bounds tend to be overoptimistic, we expect our main conclusions on the statistical significance of the estimated regression parameters to be still valid taking the full error budget into consideration.

Relative SLC patterns induced by mass variations in the Earth's system depend on (i) mass-change magnitudes, (ii) mass-change geometries, and (iii) global ice/water mass redistribution. Uniform modeling of sea-level variations is insufficient for meaningful geophysical interpretation. As such, gravitational and elastic feedback effects should always be considered. Apart from present scientific and socio-economic significance, they allow a more realistic outlook for future mid-term SLC patterns as opposed to the simplistic uniform SLC model. Our mass-balance studies over Greenland and Antarctica result in a relative SLC equivalent of  $+1.06 \pm 0.07$  mm/yr; the contribution from Antarctica is highly subject to GIA modeling.

## References

- [1] Tapley, B. D., Bettadpur, D., Ries, J. C., Thompson, P. F., Watkins, M. M. (2004): GRACE Measurements of Mass Variability in the Earth System. *Science* 305: 503-505.
- [2] Luthcke, S. B., Zwally, H. J., Abdalati, W., Rowlands, D. D., Ray, R. D., Nerem, R. S., Lemoine, F. G., McCarthy, J. J., Chinn, D. S. (2006): Recent Greenland ice mass loss by drainage system from satellite gravity observations. *Science* 314: 1286-1289.
- [3] Chen, J. L., Tapley, B. D., Wilson, C. R. (2006): Alaskan mountain glacial melting observed by satellite gravimetry. *Earth Plan. Sci. Lett.* 248: 368-378.
- [4] Velicogna, I., Wahr, J. (2006): Measurements of time-variable gravity show mass loss in Antarctica. *Science* 311: 1754-1756.
- [5] Chen, J. L., Wilson, C. R., Tapley, B. D., Blankenship, D. D., Ivins, E. R. (2007): Patagonia Icefield melting observed by Gravity Recovery and Climate Experiment (GRACE). *Geophys. Res. Lett.* 34, L22501.
- [6] Schmidt, R., Petrovic, S., Güntner, A., Barthelmes, F., Wunsch, J., Kusche, J. (2008): Periodic components of water storage changes from GRACE and global hydrology models. *J. Geophys. Res.* 113, B08419.
- [7] Wouters, B., Chambers, D., Schrama, E. J. O. (2008): GRACE observes small-scale mass loss in Greenland. *Geophys. Res. Lett.* 35, L20501.
- [8] Broeke van den, M., Bamber, J., Ettema, J., Rignot, E., Schrama, E., Berg van de, W. J., Meijgaard van, E., Velicogna, I., Wouters, B. (2009): Partitioning recent Greenland mass loss. *Science* 326: 984-986.
- [9] Baur, O., Sneeuw, N. (2011): Assessing Greenland ice mass loss by means of point-mass modeling: a viable methodology. *J. Geod.*, online first.
- [10] Velicogna, I., Wahr, J. (2006): Acceleration of Greenland ice mass loss in spring 2004. *Nature* 443: 329-331.
- [11] Baur, O., Kuhn, M., Featherstone, W. E. (2010): Linear and non-linear secular mass variations over Greenland. *Proc. VII Hotine-Marussi Symposium*, Springer, in press.
- [12] Rignot, E., Velicogna, I., Broeke van den, M., Monaghan, A., Lenaerts, J. (2011): Acceleration of the contribution of the Greenland and Antarctic ice sheets to sea level rise. *Geophys. Res. Lett.*, in press.
- [13] Lombard, A., Garcia, D., Ramillien, G., Cazenave, A., Biancale, R., Lemoine, J. M., Flechtner, F., Schmidt, R., Ishii, M. (2007): Estimation of steric sea level variations from combined GRACE and Jason-1 data. *Earth Plan. Sci. Lett.* 254: 194-202.
- [14] Farrell, W. E., Clark, J. A. (1976): On postglacial sea level. *Geophys. J. R. astr. Soc.* 46: 647-667.
- [15] Baur, O., Kuhn, M., Featherstone, W. E. (2009): GRACE-derived ice-mass variations over Greenland by accounting for leakage effects. *J. Geophys. Res.* 114, B06407.
- [16] Klemann, V., Martinec, Z. (2009): Contribution of glacial-isostatic adjustment to the geocenter. *Tectonophysics*, in press.
- [17] Quinn, K. J., Ponte, R. M. (2010): Uncertainty in ocean mass trends from GRACE. *Geophys. J. Int.* 181: 762-768.
- [18] Cheng, M., Tapley, B. D. (2004): Variations in the Earth's oblateness during the past 28 years. *J. Geophys. Res.* 109, B09402.
- [19] Wahr, J., Molenaar, M., Bryan, F. (1998): Time variability of the Earth's gravity field: Hydrological and oceanic effects and their possible detection using GRACE. *J. Geophys. Res.* 103: 30,05-30,29.
- [20] Swenson, S., Wahr, J. (2006): Post-processing removal of correlated errors in GRACE data. *Geophys. Res. Lett.* 33, L08402.
- [21] Jekeli, C. (1981): Alternative methods to smooth the Earth's gravity field. Report 327, Dept. of Geod. Sci. and Surv., Ohio State University, Columbus.
- [22] Riva, R. E. M., Gunter, B. C., Urban, T. J., Vermeersen, B. L. A., Lindenbergh, R. C., Helsen, M. M., Bamber, J. L., Wal van de, R. S. W., Broeke van den, M. R., Schutz, B. E. (2009): Glacial Isostatic Adjustment over Antarctica from combined ICESat and GRACE satellite data. *Earth Plan. Sci. Lett.* 288: 516-523.
- [23] Paulson, A., Zhong, S., Wahr, J. (2007): Inference of mantle viscosity from GRACE and relative sea level data. *Geophys. J. Int.* 171: 497-508.
- [24] Chen, J. L., Wilson, C. R., Seo, K.-W. (2009): S2 tide aliasing in GRACE time-variable gravity solutions. *J. Geod.* 83: 679-687.
- [25] Mitrova, J. X., Tamisiea, M. E., Davis, J. L., Milne, G. A. (2001): Recent mass balance of polar ice sheets inferred from patterns of global sea-level change. *Nature* 209: 1026-1029.
- [26] Kuhn, M., Featherstone, W. E., Makarynsky, O., Keller, W. (2010): Deglaciation-induced spatially variable sea level change: a simple-model case study for the Greenland and Antarctic ice sheets. *Int. J. Ocean Climate Sys.* 1(2): 67-83.

## Contacts

**Dr.-Ing. Oliver Baur**, Space Research Institute, Austrian Academy of Sciences, Schmiedlstraße 6, 8042 Graz, Austria.  
E-mail: oliver.baur@oeaw.ac.at

**Dr.-Ing. Michael Kuhn**, Western Australian Centre for Geodesy and The Institute for Geoscience Research, Curtin University of Technology, GPO Box U1987, Perth, WA 6845, Australia.  
E-mail: m.kuhn@curtin.edu.au

**Prof. Will E. Featherstone**, Western Australian Centre for Geodesy and The Institute for Geoscience Research, Curtin University of Technology, GPO Box U1987, Perth, WA 6845, Australia.  
E-mail: w.featherstone@curtin.edu.au